



Supplement of

First continuous ground-based observations of long period oscillations in the vertically resolved wind field of the stratosphere and mesosphere

Rolf Rüfenacht et al.

Correspondence to: Rolf Rüfenacht (rolf.ruefenacht@iap.unibe.ch)

The copyright of individual parts of the supplement might differ from the CC-BY 3.0 licence.

Introduction

This Supplement provides additional figures to the main article along with descriptions of these graphics. It also contains an overview of currently available wind measurement techniques and their sensitive altitude range.

Text S1. It is interesting to note that in contrast to other atmospheric layers, observations of horizontal wind between 35 and 70 km are extremely rare as illustrated by Fig. S1. The troposphere and lower stratosphere region is covered by a number of techniques such as the widely used balloon-borne radiosondes (e.g Goldberg et al., 2004), ground-based radars (e.g. Luce et al., 2001; Hooper et al., 2008) and lidars (e.g. Gentry et al., 2000). Sodar (Sonic Detection And Ranging) observations are limited to the lowermost tropospheric altitudes (e.g. Anandan et al., 2008). After its launch planned for 2016 the space-borne lidar ADM-Aeolus will provide wind data up to 26 km on a global scale (Stoffelen et al., 2006; Elfving, 2015).

Upper-atmospheric wind measurements can be provided by ground-based and space-borne airglow or absorption interferometry of atomic or molecular oxygen and hydroxyl (Gault et al., 1996a, b; Hays et al., 1993). Currently, observations from TIDI on the TIMED satellite are available for altitudes above 70 km (Killeen et al., 2006). Previously, mesospheric observations down to 65 km and stratospheric daylight wind observations up to 40 km had been performed by HRDI on UARS (Hays et al., 1993; Ortland et al., 1996). In addition, different types of ground-based radars deliver wind measurements of the upper atmosphere. Medium and low frequency radars determine wind by the drift of electron density irregularities which are sometimes detectable down to slightly below the mesopause (Briggs, 1980). Meteor radars measure the echoes from ionised particles in meteor trails drifting with the wind. Such particles are present in sufficient concentrations down to roughly 75 km (Jacobi et al., 2007). Additionally, it has been reported on the possibility of wind measurements by incoherent scatter radars reaching down to 60 km in the case of extraordinarily active auroral precipitation (Nicolls et al., 2010). Finally, ground-based lidars exploit returns from the atmospheric sodium layer to assess wind speeds between 85 and 100 km (Williams et al., 2004).

The region between 35 and 70 km where none of the previously described techniques is sensitive corresponds approximately to the so-called “radar gap” where radars do not detect usable echoes. Since the 1950ies atmospheric research rockets are used to bridge this gap by deploying falling targets to provide artificial radar backscatterers (National Research Council, 1966; Mülleman and Lübken, 2005) while wind measurements by optical tracking of a released chemical trace are generally limited to altitudes above 80 km (Larsen, 2002). However, as rocket-aided techniques are very expensive in costs they are only viable on campaign basis and

not suited for continuous monitoring. A promising technique for observations in the gap region relies on lidar systems. Souprayen et al. (1999) described a horizontal wind climatology up to 50 km whereas the first lidar wind profiles covering the entire radar gap have been reported by Baumgarten (2010). However, the only dataset published from this instrument consists of a few days of polar night profiles (see also Hildebrand et al., 2012). Sensitivity of infrasound observations to the middle-atmospheric wind has been reported (e.g. Le Pichon et al., 2005a, b; Assink et al., 2014), but no full retrievals quantifying the wind speeds have yet been provided.

Microwave radiometry is sensitive to atmospheric emissions originating from the altitude range between 35 and 70 km where wind measurements are extremely scarce. This technique has a long history in measuring volume mixing ratio profiles of trace gases such as ozone or water vapor at these altitudes (e.g. Lobsiger et al., 1984; Lobsiger, 1987; Nedoluha et al., 1995, and references therein). Back in 1993 already, Clancy and Muhlemann (1993) had proposed the application of microwave radiometry for wind measurements in the middle atmosphere. One decade later Burrows (2007) and Flury et al. (2008) delivered the practical proof of the feasibility of such observations by measurements with an antarctic CO telescope and an airborne water vapour radiometer. These publications presented short data sets of average middle-atmospheric winds, whereas Rüfenacht et al. (2012) first reported on measurements of vertically resolved wind profiles in the upper stratosphere and mesosphere by a microwave radiometer operated as part of a regular measurement regime. Baron et al. (2013) later presented a data set comprising seven months of space-borne wind profile observations from SMILES. Unluckily, a technical failure stopped the operation of this instrument a few months before the ground-based wind radiometer WIRA recorded its first atmospheric observations so that there is no possibility for intercomparisons between the two instruments. Before the launch of SMILES, Wu et al. (2008) had described an approach for the retrieval of mesopause region wind profiles from the microwave limb sounder (MLS) on AURA.

Text S2. Figures. S3 and S4 are analogs of Figs. 2 and 5 in the main article except that a pseudo-wavelet approach similar to the methods used in Studer et al. (2012) and Scheiben et al. (2014) was applied for the periodogram calculation. However, in the case of wind measurements, longer data gaps are present in the time series at some altitudes, therefore a more thorough treatment of those is necessary. Unlike in the cited studies data gaps were treated as missing values instead of being interpolated. Comparing Figs. S3 and S4 to Figs. 2 and 5 reveals only minor differences, hence both, the pseudo-wavelet and the Lomb-Scargle approach are suited for the spectral analysis of microwave remote sensing data.

Text S3. Figures S5 to S12 show the periodograms of unaltered ECMWF data for all campaign sites and all time periods covered by the present study. Each figure covers the time interval of one measurement campaign. This additional data allows to better discriminate seasonal and latitude dependent effects from randomly occurring features.

Text S4. Figure S13 presents the temporal evolution of the periodograms of WIRA data at the 0.05 hPa level. This corresponds to the altitude where Fig. 2 in the main article shows a minimum in the oscillation activity.

Text S5. Fig. S14 shows the campaign averages of the altitude dependent periodograms divided by the mean wind profile of the respective campaign for selected locations. Only zonal wind data from Bern, Sodankylä and Provence have been used because the average zonal wind component from La Réunion as well as the average meridional components from Provence and La Réunion are close to zero so that a normalization would yield meaningless results. The agreement between ECMWF and WIRA becomes very good also for the upper altitudes when the periodogram is normalized by the average wind profile. This implies that the absolute wind speed discrepancy described in Rüfenacht et al. (2014) and the oscillation amplitude discrepancy increase in the same manner with increasing altitude.

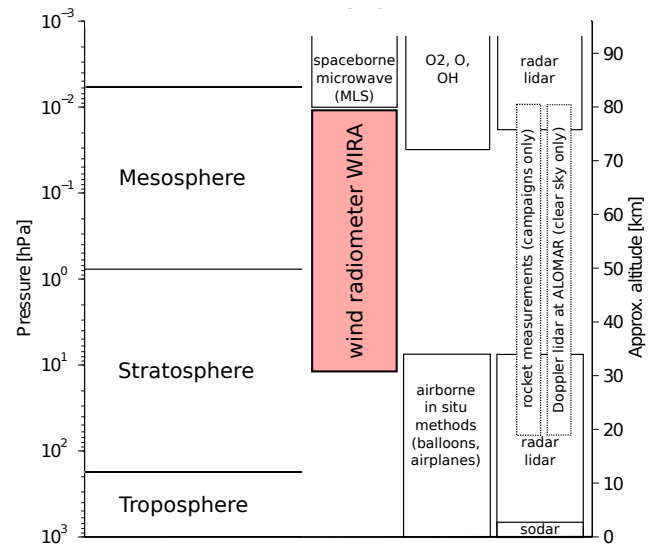


Figure S1. Overview of the existing techniques for wind observations with their typical sensitive altitude range. Under special atmospheric conditions extensions of the lower altitude limit of upper atmospheric incoherent scatter radars down to 60 km have been reported.

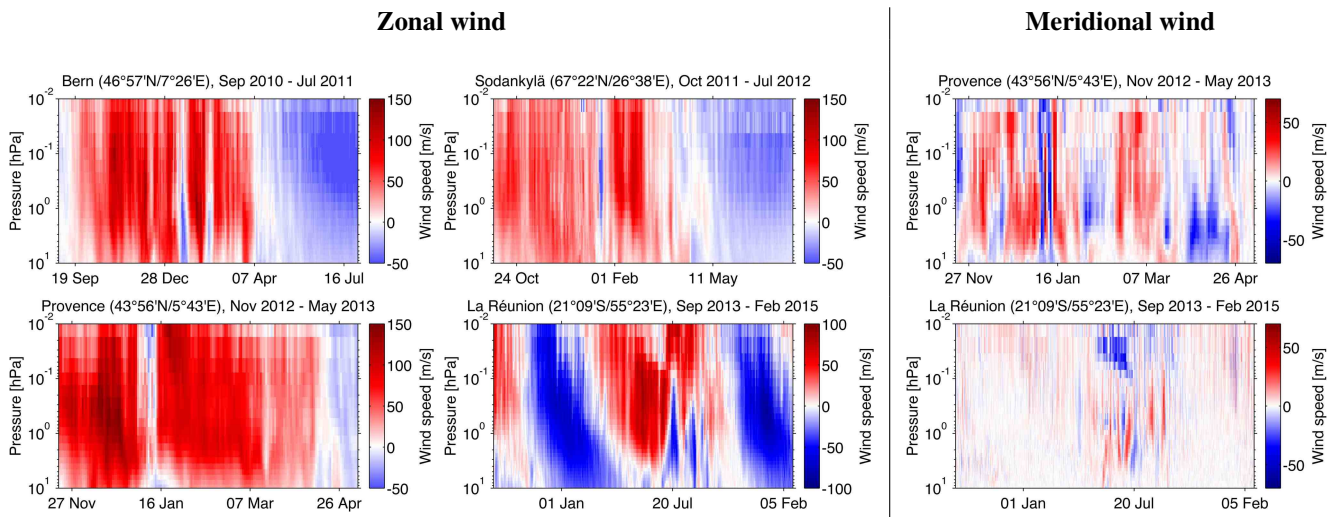


Figure S2. As Fig. 1 in the main article but for wind data from the ECMWF Operational Analysis.

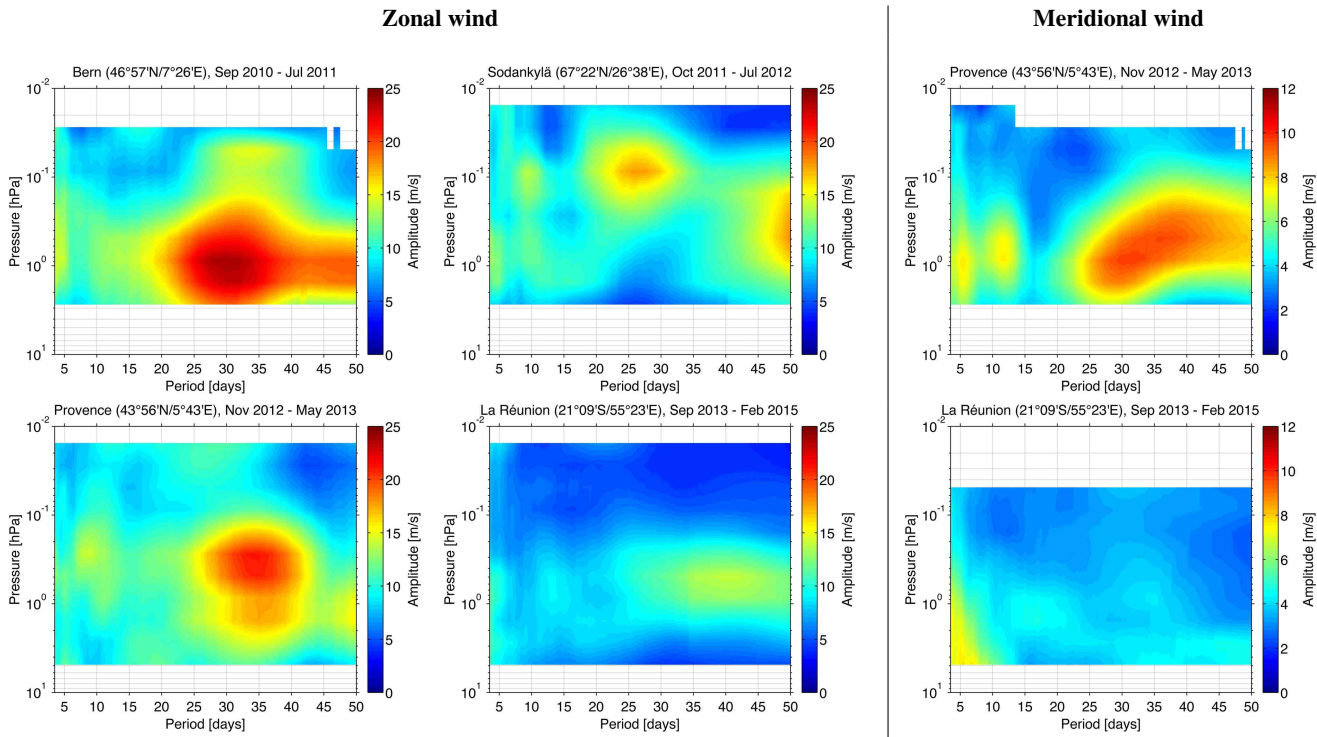


Figure S3. As Fig. 2 in the main article but for results obtained with the pseudo-wavelet approach.

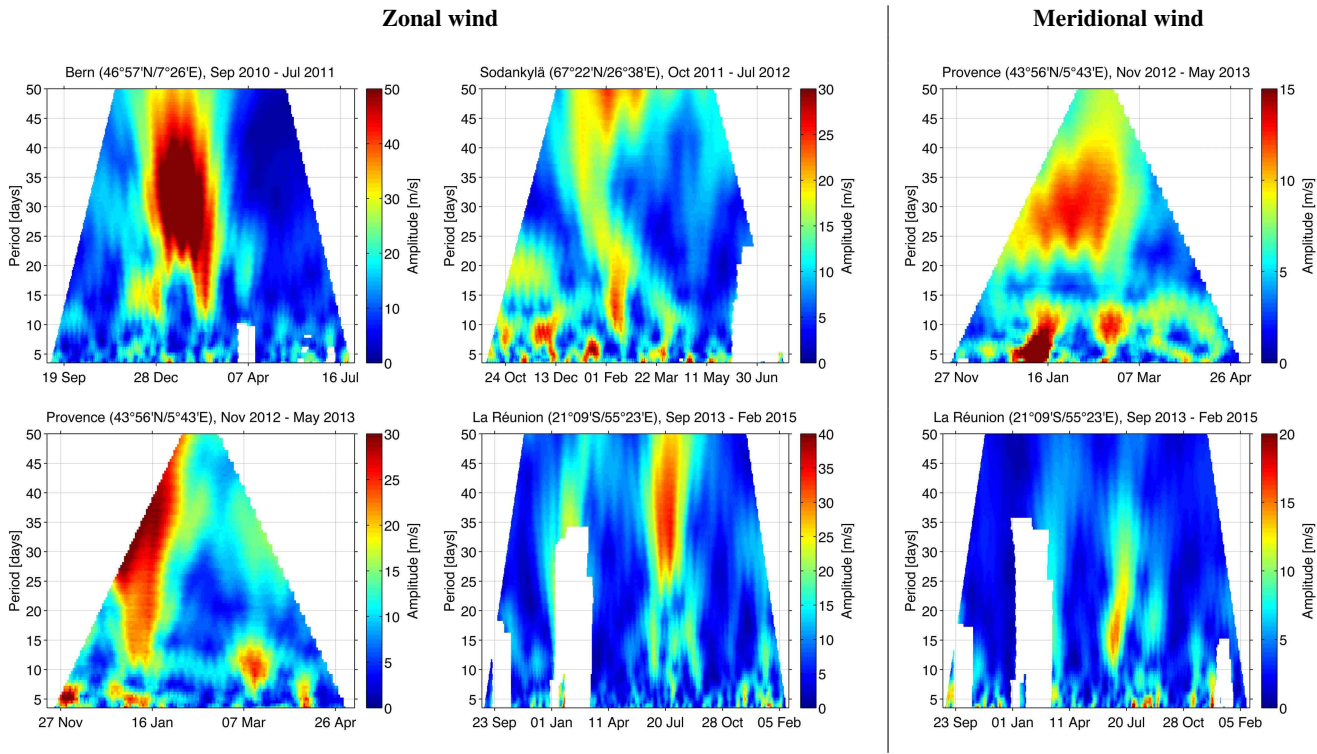


Figure S4. As Fig. 5 in the main article but for results obtained with the pseudo-wavelet approach.

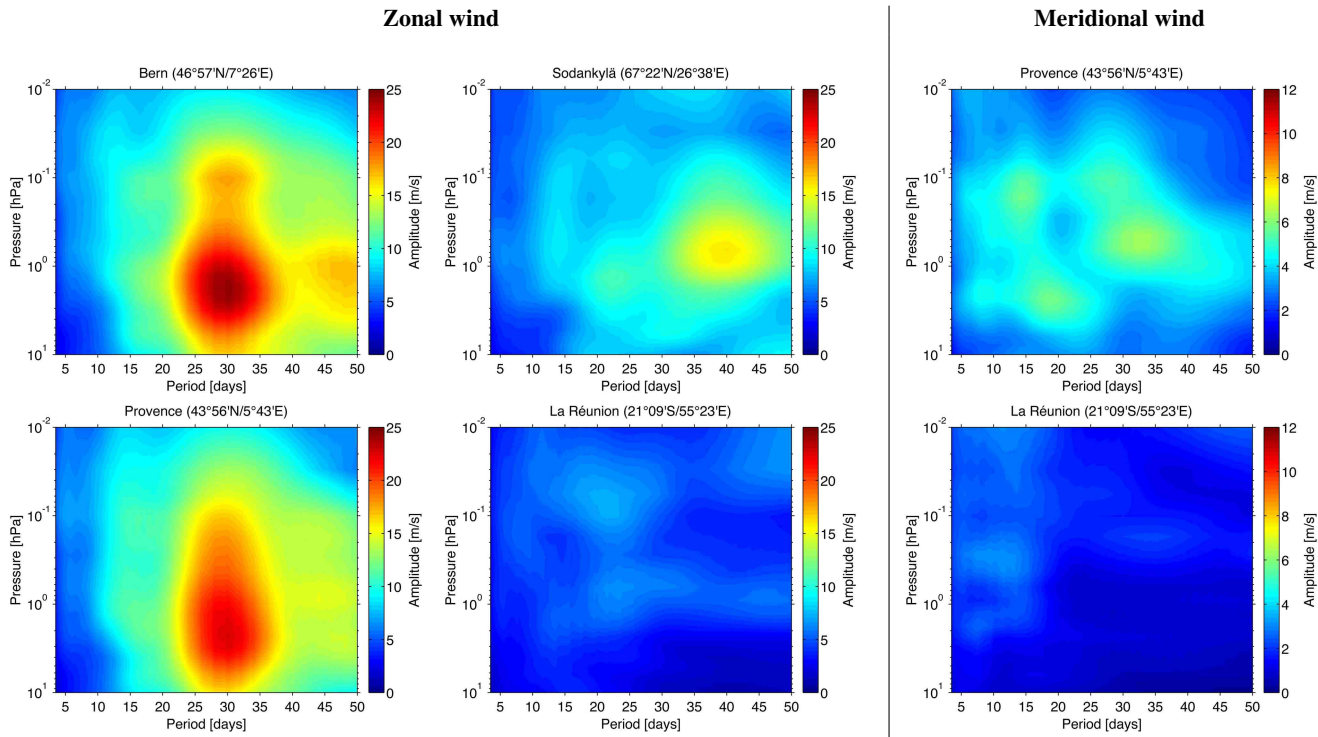


Figure S5. As Fig. 4 in the main article but with data for the time period 1 Sep 2010 - 31 Jul 2011 (time of the Bern campaign) for all locations.

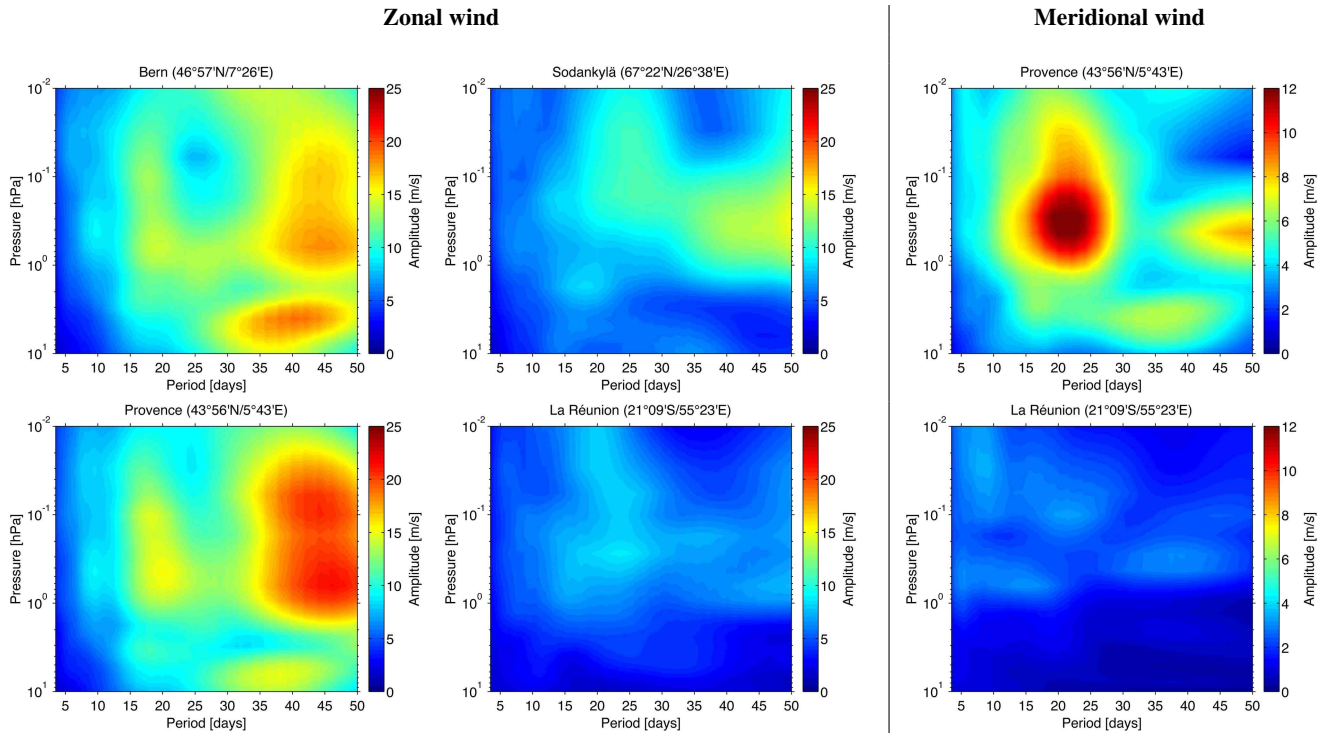


Figure S6. As Fig. 4 in the main article but with data for the time period 1 Oct 2011 - 31 Jul 2012 (time of the Sodankylä campaign) for all locations.

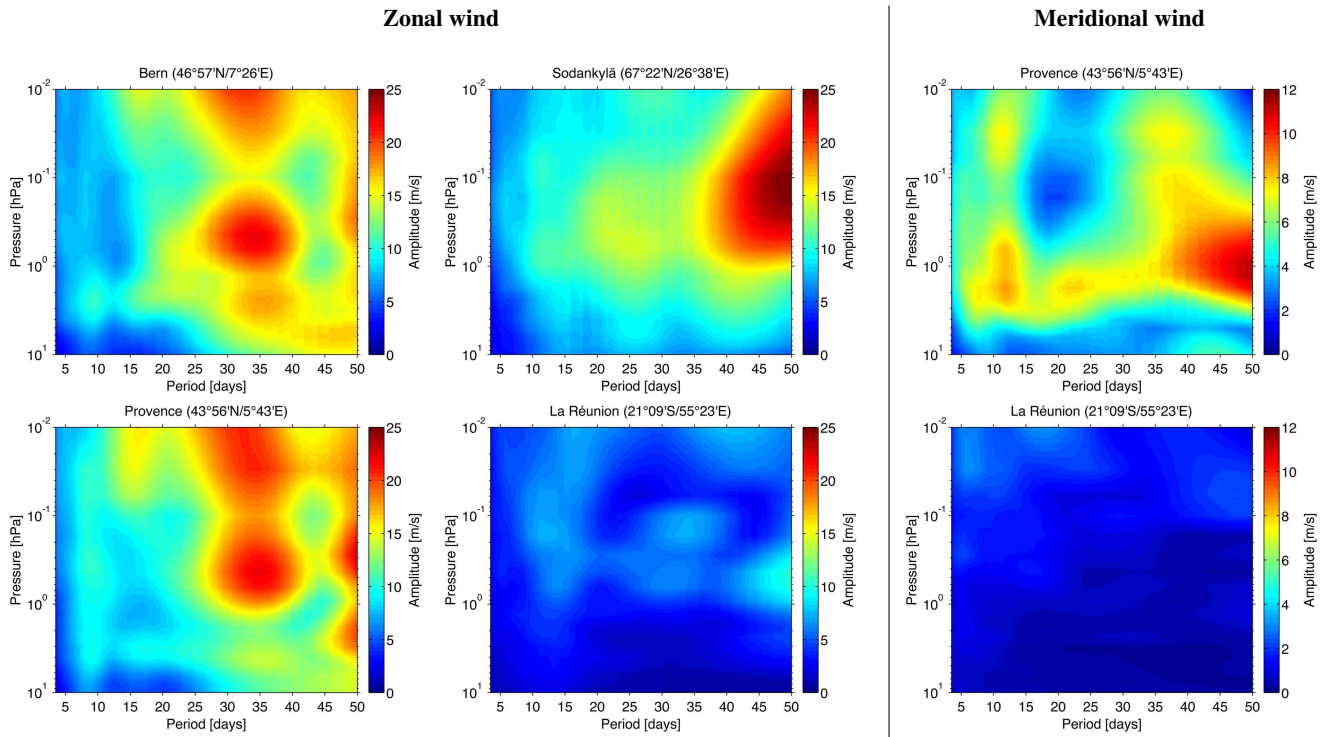


Figure S7. As Fig. 4 in the main article but with data for the time period 20 Nov 2012 - 6 May 2013 (time of the Provence campaign) for all locations.

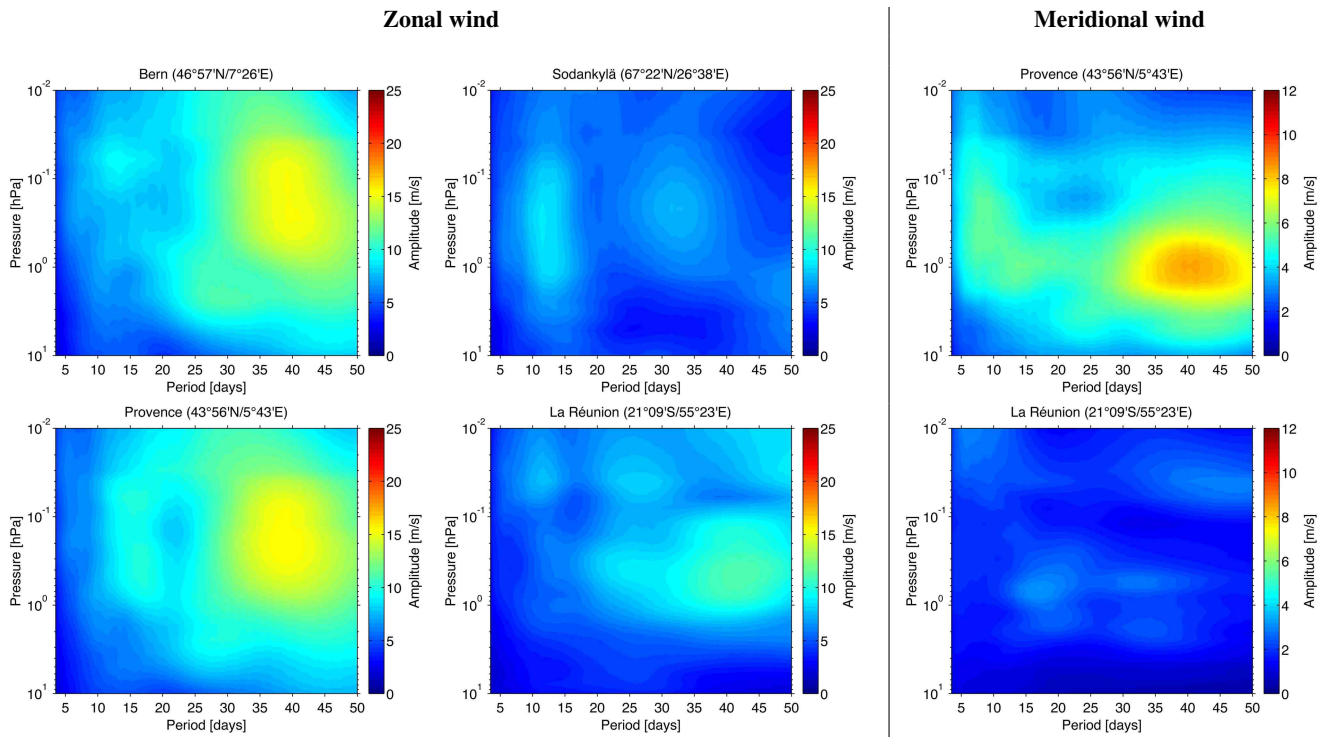


Figure S8. As Fig. 4 in the main article but with data for the time period 1 Sep 2013 - 21 Feb 2015 (time of the La Réunion campaign) for all locations.

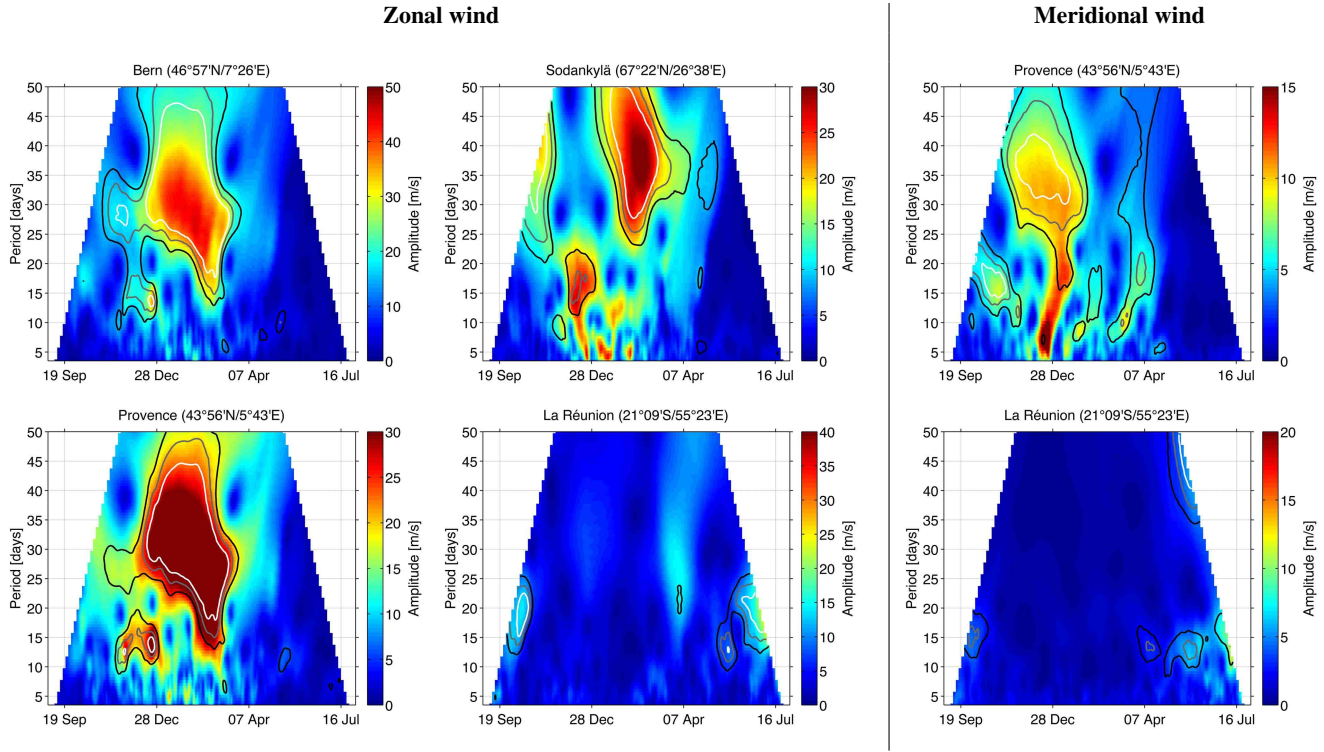


Figure S9. As Fig. 7 in the main article but with data for the time period 1 Sep 2010 - 31 Jul 2011 (time of the Bern campaign) for all locations.

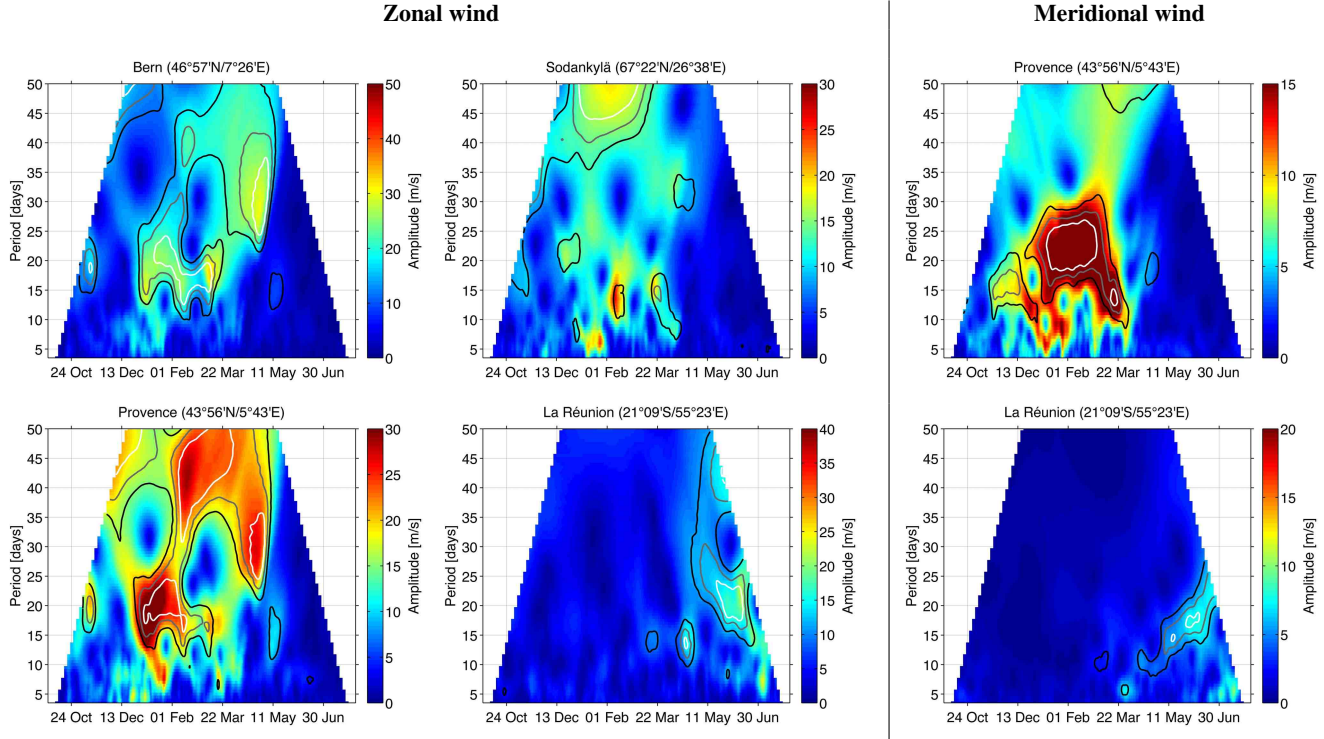


Figure S10. As Fig. 7 in the main article but with data for the time period 1 Oct 2011 - 31 Jul 2012 (time of the Sodankylä campaign) for all locations.

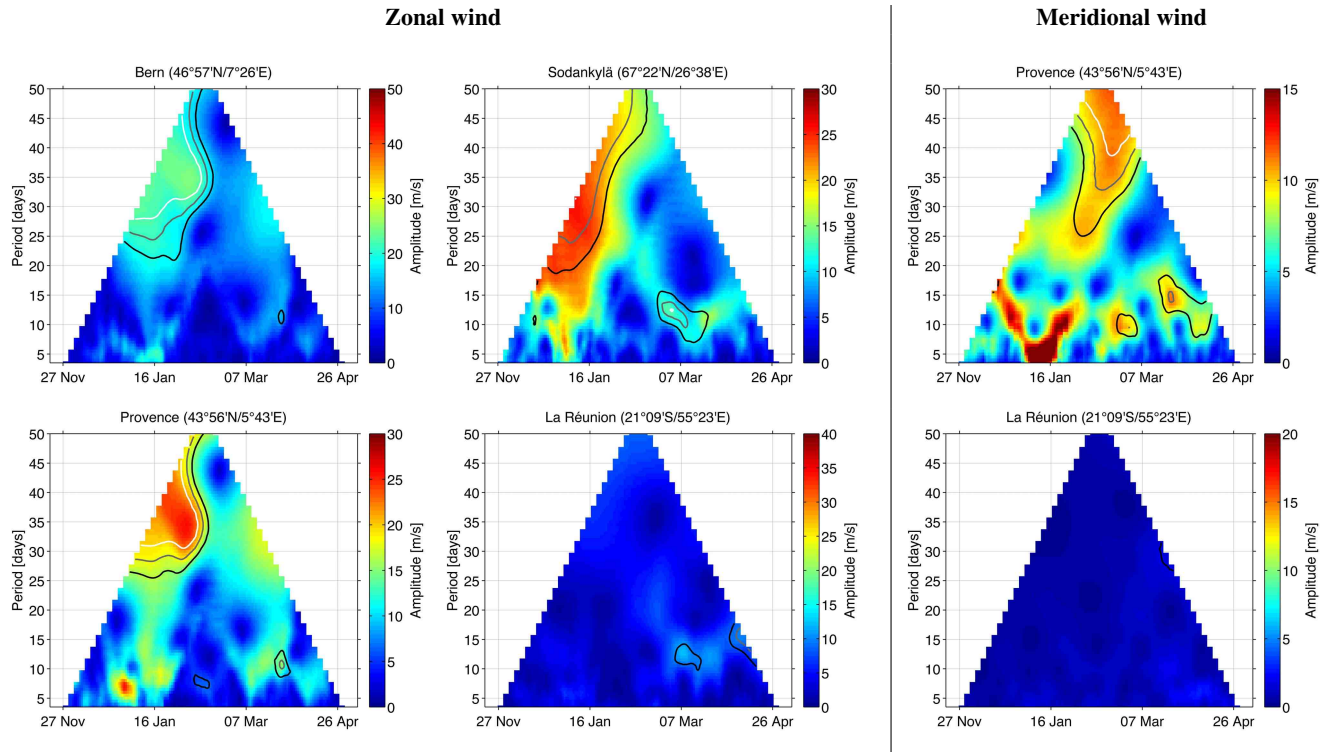


Figure S11. As Fig. 7 in the main article but with data for the time period 20 Nov 2012 - 6 May 2013 (time of the Provence campaign) for all locations.

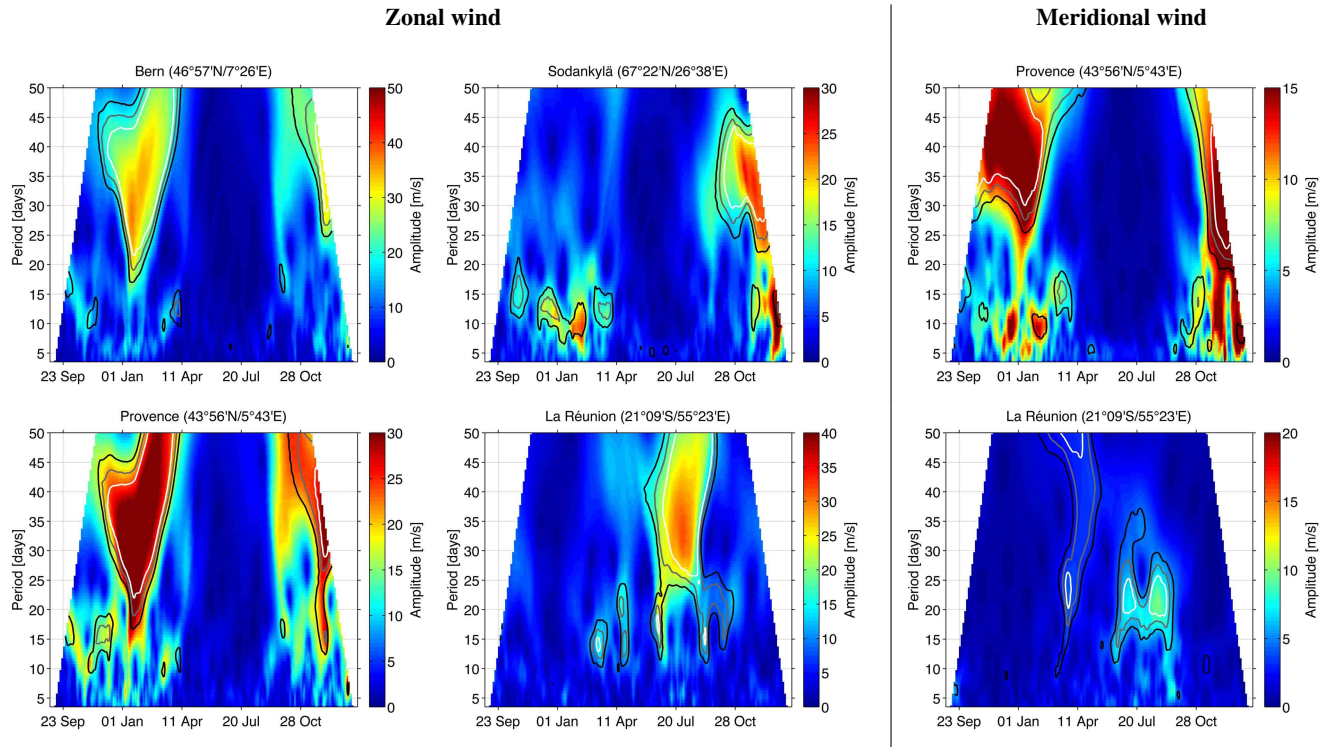


Figure S12. As Fig. 7 in the main article but with data for the time period 1 Sep 2013 - 21 Feb 2015 (time of the La Réunion campaign) for all locations.

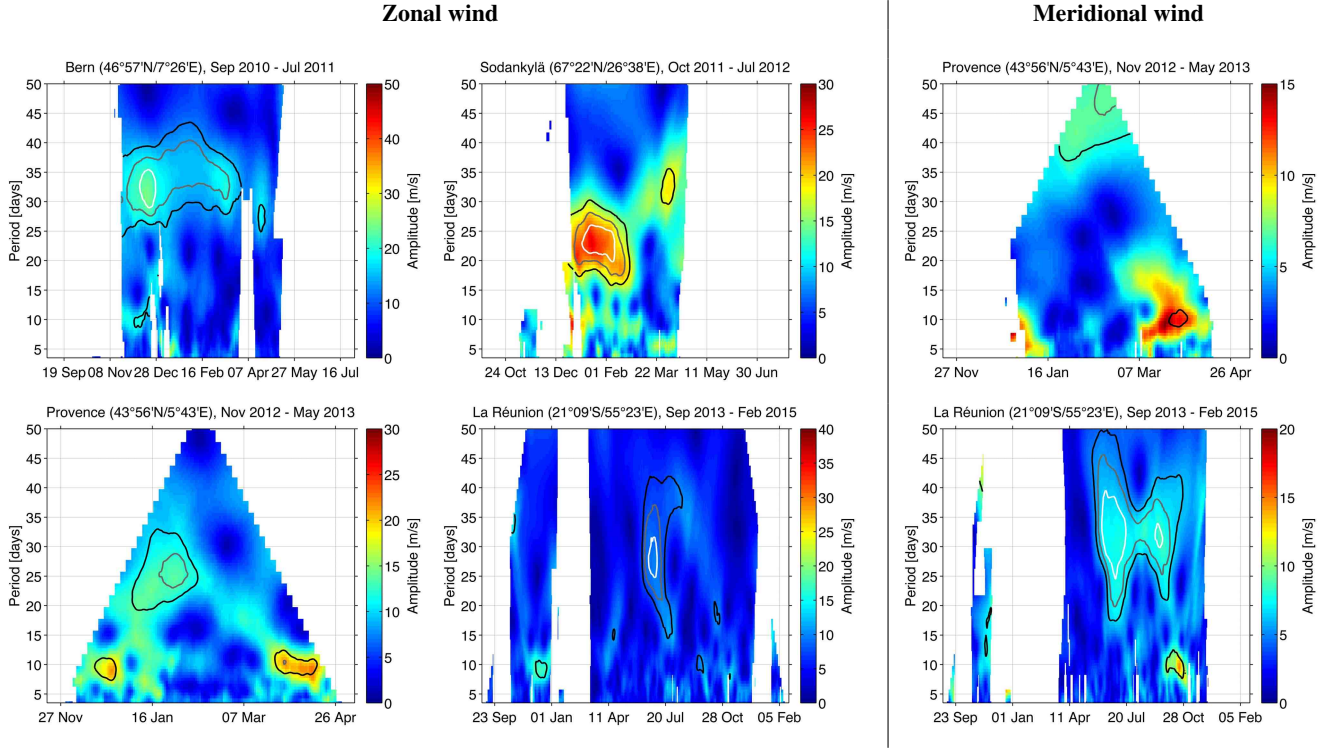


Figure S13. As Fig. 5 in the main article but for the temporal evolution of the WIRA periodogram at 0.05 hPa, which roughly corresponds to the altitude of minimal oscillation amplitudes. The color scale is identical to the plots at stratopause level.

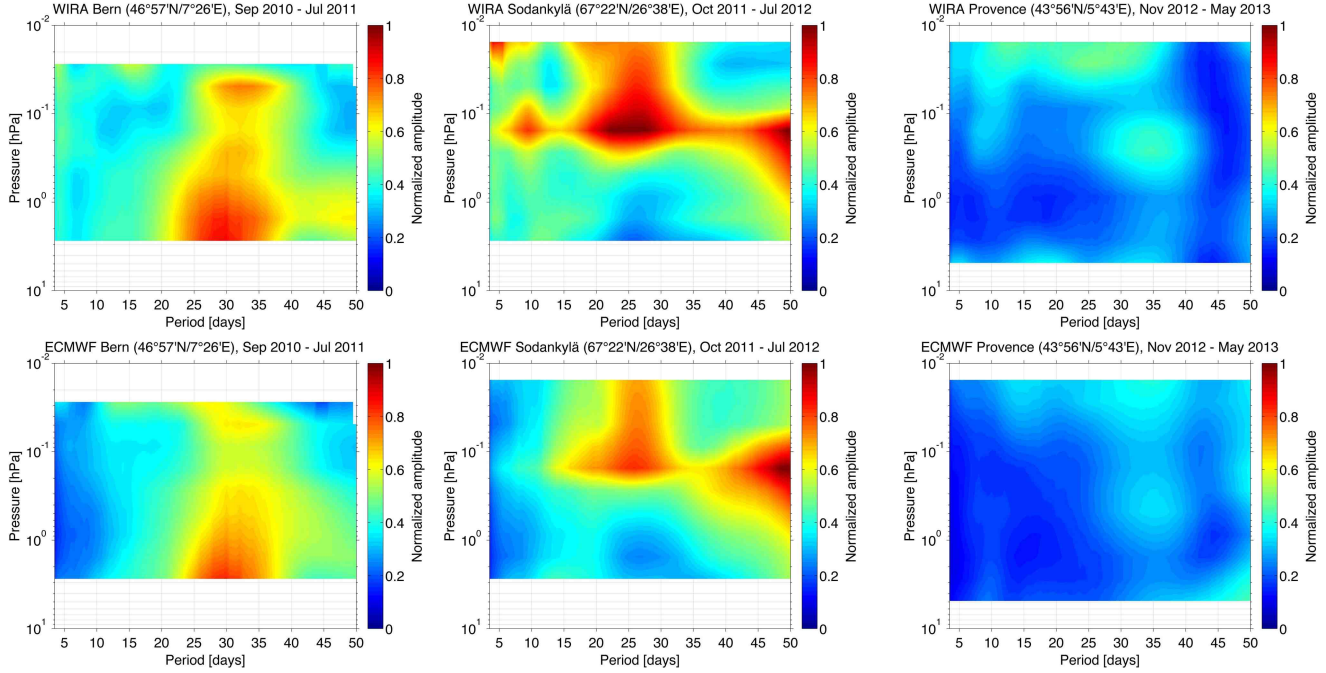


Figure S14. Temporally averaged periodograms of zonal and meridional wind profiles divided by the temporal average wind profile for the respective measurement campaigns. Results are shown for the zonal wind component in Bern, Sodankylä and Provence. Upper panels: WIRA; lower panels: ECMWF at WIRA.

References

- Anandan, V. K., Kumar, M. S., and Rao, I. S.: First Results of Experimental Tests of the Newly Developed NARL Phased-Array Doppler Sodar, *J. Atmos. Ocean. Technol.*, 25, 1778–1784, doi:10.1175/2008JTECHA1050.1, 2008.
- Assink, J. D., Pichon, A. L., Blanc, E., Kallel, M., and Khemiri, L.: Evaluation of wind and temperature profiles from ECMWF analysis on two hemispheres using volcanic infrasound, *J. Geophys. Res.-Atmos.*, 119, 8659–8683, doi:10.1002/2014JD021632, 2014.
- Baron, P., Murtagh, D. P., Urban, J., Sagawa, H., Ochiai, S., Kasa, Y., Kikuchi, K., Khosrawi, F., Körnich, H., Mizobuchi, S., Sagi, K., and Yasui, M.: Observation of horizontal winds in the middle-atmosphere between 30° S and 55° N during the northern winter 2009–2010, *Atmos. Chem. Phys.*, 13, 6049–6064, doi:10.5194/acp-13-6049-2013, 2013.
- Baumgarten, G.: Doppler Rayleigh/Mie/Raman lidar for wind and temperature measurements in the middle atmosphere up to 80 km, *Atmos. Meas. Tech.*, 3, 1509–1518, doi:10.5194/amt-3-1509-2010, 2010.
- Briggs, B. H.: Radar observations of atmospheric winds and turbulence - a comparison of techniques, *J. Atmos. Sol.-Terr. Phys.*, 42, 823–833, doi:10.1016/0021-9169(80)90086-0, 1980.
- Burrows, S. M.: High-latitude remote sensing of mesospheric wind speeds and carbon monoxide, *J. Geophys. Res.-Atmos.*, 112, doi:10.1029/2006JD007993, 2007.
- Clancy, R. and Muhlemann, D.: Ground-based microwave spectroscopy of the Earth's stratosphere and mesosphere, in: Atmospheric Remote Sensing by Microwave Radiometry, edited by Janssen, M. A., chap. 7, pp. 372–374, John Wiley, 1993.
- Elfving, A.: Aeolus – ESA's Wind Lidar Mission: Objectives, Design & Latest Results, Talk at Aeolus Cal/Val Workshop, 2015.
- Flury, T., Hocke, K., Müller, S., and Kämpfer, N.: First measurements of lower mesospheric wind by airborne microwave radiometry, *Geophys. Res. Lett.*, 35, doi:10.1029/2008GL034663, 2008.
- Gault, W. A., Brown, S., Moise, A., Liang, D., Sellar, G., Shepherd, G. G., and Wimperis, J.: ERWIM: An E-region wind interferometer, *Appl. Optics*, 35, 2913–2922, doi:10.1364/AO.35.002913, 1996a.
- Gault, W. A., Thuillier, G., Shepherd, G. G., Zhang, S. P., Wiens, R. H., Ward, W. E., Tai, C., Solheim, B. H., Rochon, Y. J., McLandress, C., Lathuillere, C., Fauliot, V., Herse, M., Hersom, C. H., Gattinger, R., Bourg, L., Burrage, M. D., Franke, S. J., Hernandez, G., Manson, A., Niciejewski, R., and Vincent, R. A.: Validation of O(S-1) wind measurements by WINDII: The WIND imaging interferometer on UARS, *J. Geophys. Res.-Atmos.*, 101, 10 405–10 430, doi:10.1029/95JD03352, 1996b.
- Gentry, B. M., Chen, H. L., and Li, S. X.: Wind measurements with 355-nm molecular Doppler lidar, *Opt. Lett.*, 25, 1231–1233, doi:10.1364/OL.25.001231, 2000.
- Goldberg, R. A., Fritts, D. C., Williams, B. P., Lübken, F.-J., Rapp, M., Singer, W., Latteck, R., Hoffmann, P., Mullemann, A., Baumgarten, G., Schmidlin, F.-J., She, C., and Krueger, D. A.: The MaCWave/MIDAS rocket and ground-based measurements of polar summer dynamics: Overview and mean state structure, *Geophys. Res. Lett.*, 31, doi:10.1029/2004GL019411, 2004.
- Hays, P. B., Abreu, V. J., Dobbs, M. E., Gell, D. A., Grassl, H. J., and Skinner, W. R.: The high-resolution doppler imager on the Upper Atmosphere Research Satellite, *J. Geophys. Res.-Atmos.*, 98, 10 713–10 723, doi:10.1029/93JD00409, 1993.
- Hildebrand, J., Baumgarten, G., Fiedler, J., Hoppe, U.-P., Kaifler, B., Lübken, F.-J., and Williams, B. P.: Combined wind measurements by two different lidar instruments in the Arctic middle atmosphere, *Atmos. Meas. Tech.*, 5, 2433–2445, doi:10.5194/amt-5-2433-2012, 2012.
- Hooper, D. A., Nash, J., Oakley, T., and Turp, M.: Validation of a new signal processing scheme for the MST radar at Aberystwyth, *Ann. Geophys.*, 26, 3253–3268, doi:10.5194/angeo-26-3253-2008, 2008.
- Jacobi, C., Froehlich, K., Viehweg, C., Stober, G., and Kuerschner, D.: Midlatitude mesosphere/lower thermosphere meridional winds and temperatures measured with meteor radar, *Adv. Space Res.*, 39, 1278–1283, doi:10.1016/j.asr.2007.01.003, 2007.
- Killeen, T. L., Wu, Q., Solomon, S. C., Ortland, D. A., Skinner, W. R., Niciejewski, R. J., and Gell, D. A.: TIMED Doppler interferometer: Overview and recent results, *J. Geophys. Res.-Space*, 111, doi:10.1029/2005JA011484, 2006.
- Larsen, M. F.: Winds and shears in the mesosphere and lower thermosphere: Results from four decades of chemical release wind measurements, *J. Geophys. Res.-Space*, 107, SIA 28–1–SIA 28–14, doi:10.1029/2001JA000218, 2002.
- Le Pichon, A., Blanc, E., and Drob, D.: Probing high-altitude winds using infrasound, *J. Geophys. Res.-Atmos.*, 110, doi:10.1029/2005JD006020, 2005a.
- Le Pichon, A., Blanc, E., Drob, D., Lambotte, S., Dessa, J. X., Lardy, M., Bani, P., and Vergniolle, S.: Infrasound monitoring of volcanoes to probe high-altitude winds, *J. Geophys. Res.-Atmos.*, 110, doi:10.1029/2004JD005587, 2005b.
- Lobsiger, E.: Ground-based microwave radiometry to determine stratospheric and mesospheric ozone profiles, *J. Atmos. Terr. Phys.*, 49, 493–501, doi:10.1016/0021-9169(87)90043-2, 1987.
- Lobsiger, E., Künzi, K. F., and Dütsch, H. U.: Comparison of stratospheric ozone profiles retrieved from microwave-radiometer and Dobson-spectrometer data, *J. Atmos. Terr. Phys.*, 46, 799–806, doi:10.1016/0021-9169(84)90060-6, 1984.
- Luce, H., Fukao, S., Yamamoto, M., Sidi, C., and Dalaudier, F.: Validation of winds measured by MU radar with GPS radiosondes during the MUTSI campaign, *J. Atmos. Ocean. Technol.*, 18, 817–829, doi:10.1175/1520-0426(2001)018<0817:VOWMBM>2.0.CO;2, 2001.
- Müllemann, A. and Lübken, F.-J.: Horizontal winds in the mesosphere at high latitudes, *Adv. Space Res.*, 35, 1890–1894, doi:10.1016/j.asr.2004.11.014, Coupling Processes in the MLT Region, 2005.
- National Research Council: United States Space Science Program: Report to COSPAR, Ninth Meeting, National Academy of Sciences, 1966.
- Nedoluha, G. E., Bevilacqua, R. M., Gomez, R. M., Thacker, D. L., Waltman, W. B., and Pauls, T. A.: Ground-based measurements of water vapor in the middle atmosphere, *J. Geophys. Res.-Atmos.*, 100, 2927–2939, doi:10.1029/94JD02952, 1995.
- Nicolls, M. J., Varney, R. H., Vadas, S. L., Stamus, P. A., Heinzelman, C. J., Cosgrove, R. B., and Kelley, M. C.: Influence of an inertia-gravity wave on mesospheric dynamics: A case study with the Poker Flat Incoherent Scatter Radar, *J. Geophys. Res.-*

- Atmos., 115, doi:10.1029/2010JD014042, 2010.
- Ortland, D. A., Skinner, W. R., Hays, P. B., Burrage, M. D., Lieberman, R. S., Marshall, A. R., and Gell, D. A.: Measurements of stratospheric winds by the high resolution Doppler imager, Journal of Geophysical Research: Atmospheres, 101, 10 351–10 363, doi:10.1029/95JD02142, <http://dx.doi.org/10.1029/95JD02142>, 1996.
- Rüfenacht, R., Murk, A., Kämpfer, N., Eriksson, P., and Buehler, S. A.: Middle-atmospheric zonal and meridional wind profiles from polar, tropical and midlatitudes with the ground-based microwave Doppler wind radiometer WIRA, *Atmos. Meas. Tech.*, 7, 4491–4505, doi:10.5194/amt-7-4491-2014, 2014.
- Rüfenacht, R., Kämpfer, N., and Murk, A.: First middle-atmospheric zonal wind profile measurements with a new ground-based microwave Doppler-spectro-radiometer, *Atmos. Meas. Tech.*, 5, 2647–2659, doi:10.5194/amt-5-2647-2012, 2012.
- Scheiben, D., Tschanz, B., Hocke, K., Kämpfer, N., Ka, S., and Oh, J. J.: The quasi 16-day wave in mesospheric water vapor during boreal winter 2011/2012, *Atmos. Chem. Phys.*, 14, 6511–6522, doi:10.5194/acp-14-6511-2014, 2014.
- Souprayen, C., Garnier, A., Hertzog, A., Hauchecorne, A., and Porteneuve, J.: Rayleigh-Mie Doppler wind lidar for atmospheric measurements. Instrumental setup, validation, and first climatological results, *Appl. Optics*, 38, 2410–2421, doi:10.1364/AO.38.002410, 1999.
- Stoffelen, A., Marseille, G. J., Bouttier, F., Vasiljevic, D., de Haan, S., and Cardinali, C.: ADM-Aeolus Doppler wind lidar Observing System Simulation Experiment, *Q. J. Roy. Meteor. Soc.*, 132, 1927–1947, doi:10.1256/qj.05.83, 2006.
- Studer, S., Hocke, K., and Kämpfer, N.: Intraseasonal oscillations of stratospheric ozone above Switzerland, *J. Atmos. Sol.-Terr. Phys.*, 74, 189 – 198, doi:10.1016/j.jastp.2011.10.020, 2012.
- Williams, B. P., Fritts, D. C., Wang, L., She, C.-Y., Vance, J. D., Schmidlin, F. J., Goldberg, R. A., Mullemann, A., and Lübken, F.-J.: Gravity waves in the arctic mesosphere during the MaCWave/MIDAS summer rocket program, *Geophys. Res. Lett.*, 31, doi:10.1029/2004GL020049, 2004.
- Wu, D. L., Schwartz, M. J., Waters, J. W., Limpasuvan, V., Wu, Q., and Killeen, T. L.: Mesospheric Doppler wind measurements from Aura Microwave Limb Sounder (MLS), *Adv. Space Res.*, 42, 1246–1252, doi:10.1016/j.asr.2007.06.014, 2008.